Beam Dynamics in a Hybrid Standing Wave-Traveling Wave Photoinjector

J. Rosenzweig[€], D. Alesini[¥], A. Boni[€], M. Ferrario[¥], A. Fukusawa[€], A. Mostacci[$], B. O'Shea[€], L. Palumbo[$], B. Spataro[¥]

[€]*UCLA Dept. of Physics and Astronomy, 405 Hilgard Ave., Los Angeles, CA 90034, USA*
[$]*Dipartimento di Energetica, Universita degli Studi di Roma "La Sapienza", 00161 Roma (RM) Italy*
[¥] *Laboratari Nazionali di Frascati, Istituto Nazionale di Fisica Nucleare, 00044 Frascati (RM) Italy*

Abstract. We discuss the dynamics of of a photoinjector beam in a hybrid traveling wave-standing wave photoinjector. With the field profile deduced from electromagnetic simulations, it is seen that the acceleration program induces strong velocity bunching. The beam dynamics in this scenario are explored using UCLA PARMELA. With a solenoid field overlaid on the TW section one may control emittance oscillations during bunching and acceleration. It is seen that the S-band device currently under development at UCLA may produce a 1 nC, 21 MeV, 100 micron rms pulse length beam, with emittance of 3 mm-mrad. Applications of this beam for creating coherent radiation are discussed.

Keywords: photoinjector, traveling wave, standing wave, emittance, space-charge, radiation.
PACS: 52.59.Rz, 41.75.Fr, 52.59.Sa, 41.60.Bq

INTRODUCTION

It has been known for some time that the scaling laws derived from inherent dynamical considerations[1] would indicate that the brightness of RF photoinjectors should improve with higher frequency operation, $B = 2I/\varepsilon_n^2 \propto \lambda_{RF}^{-2}$. As the electric field in the device must also scale as $E \propto \lambda_{RF}^{-1}$, scaling of the standard > 100 MV/m high gradient S-band gun[2] would give unrealistically high electric field. Thus one is should consider to integrated photoinjectors[3], which combine the "gun" section (emission/capture of the beam to ~4 MeV) with post-acceleration (in the "linac") to above 10 MeV.

This has been accomplished in 10-12 cell standing wave (SW) structures, such as the S-band plane wave transformer at UCLA[4]. In the PWT case, one attempts to provide as much mode separation as possible through use of a strongly cell-cell coupled structure design that implies a nearly flat acceleration field profile as a function of z in the injector, and that uses cooling methods that do not scale well with increased RF frequency. In addition, as they are SW devices, one must contend with large reflected power. Thus, while the PWT (and related devices such as the LANL L-band integrated injector) is a robust system, it has several drawbacks. The first is related to the field flatness — the accelerating gradient set by cathode field requirements is not diminished in the post-acceleration section. This produces both non-ideal emittance compensation conditions and, perhaps more importantly, the RF

power is not efficiently used to obtain large total energy gain. Because of these problems, the proposed scaling of the PWT to X-band was not ultimately brought to fruition[5].

An alternative structure, originally proposed at UCLA[6], has been undergoing strong development at UCLA and Universita degli Studi di Roma "La Sapienza" (URLS), termed the *hybrid* standing wave/traveling wave injector. This device is coupled to waveguide input power in the third cell, with axial coupling feeding the upstream standing wave higher gradient "gun" section, and the long, lower gradient, downstream traveling wave post-acceleration section, as shown in Fig. 1.

RF CHARACTERISTICS OF THE HYBRID PHOTOINJECTOR

The microwave circuitry of this device was studied originally in a Phase I SBIR project by a UCLA and its industrial collaborator, Xgamma, Inc. With the industrial component leaving the project, UCLA and URLS, as well as INFN-LNF (Frascati), are now collaborating on the 3D microwave modeling of the hybrid photoinjector, as part of a larger collaboration on advanced RF devices (e.g. RF deflectors for beam diagnostics, and the SPARC RF photoinjector). These studies are proceeding in both S-band (at UCLA) and X-band (URLS), with the aim to take advantage of existing RF power sources and testing equipment at both institutions. It should be noted that, with its strong applications to high gradient X-band RF power research, this project has been included in the recently formed US High Gradient RF Structure collaboration.

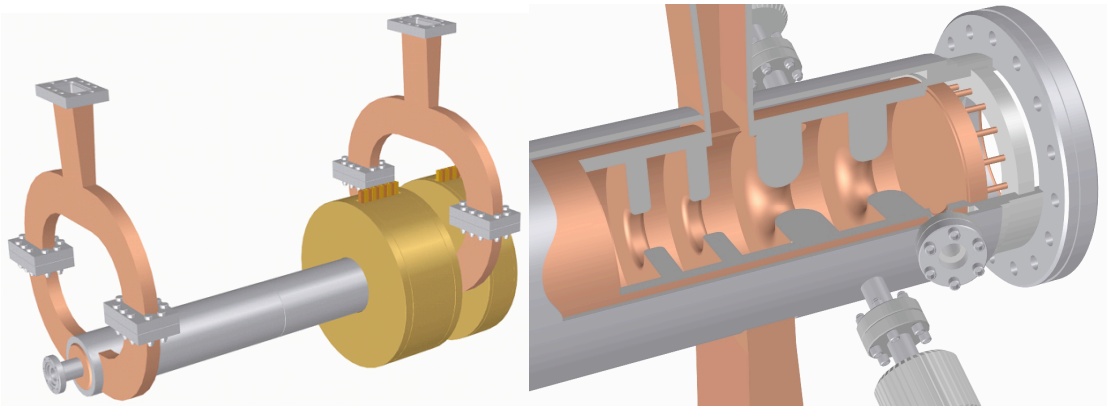

Figure 1. (left) Hybrid standing/traveling wave RF photoinjector rendered design, including couplers and solenoids; (right) cutaway of coupling region, showing gun-type region with cathode.

The major advantages of this device are, from RF viewpoint, lack of significant reflection — eliminating the need for an expensive or challenging circulator/isolator — and simpler, more efficient use of RF power. With the low gradient traveling wave section, one may achieve nearly a much higher eventual beam energy with the available RF power. From the output beam standpoint, simulation of this design shows flexibility in achieving excellent emittance performance at higher energy, and with lower cost.

From the viewpoint of high frequency RF (in *e.g.* the CLIC context), this project

also presents several unique opportunities. As a new type of RF structure, a fundamental theoretical and computational understanding of the device is desirable, particularly in regards to understanding and optimizing couplers. Further, the gun section of the device is inherently high gradient at the RF frequencies of interest — the *lowest* peak on-axis field in an X-band hybrid photoinjector currently under study is 240 MV/m. Thus the eventual high power (~30-45 MW) testing of this structure would indeed be at a field level with relevance to the basic high gradient RF photoinjector research. This component of the project is centered at Roma/Frascati, where the X-band RF infrastructure is under development, including methods of fabricating and joining the structures, such as brazing and electroforming.

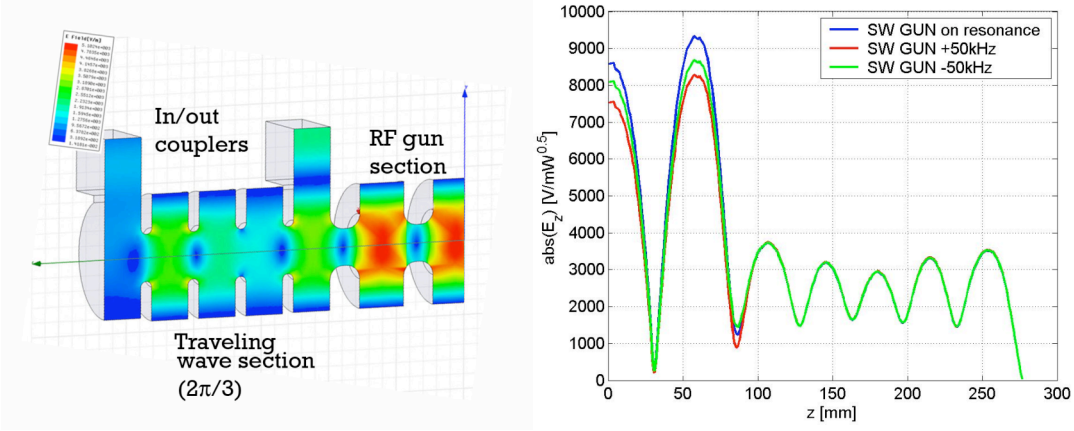

Figure 2. (left) HFSS model of hybrid photoinjector under study at UCLA; (right) Field map of photoinjector model, includng input/output coupler, coupling cell, and 2π/3 mode TW section.

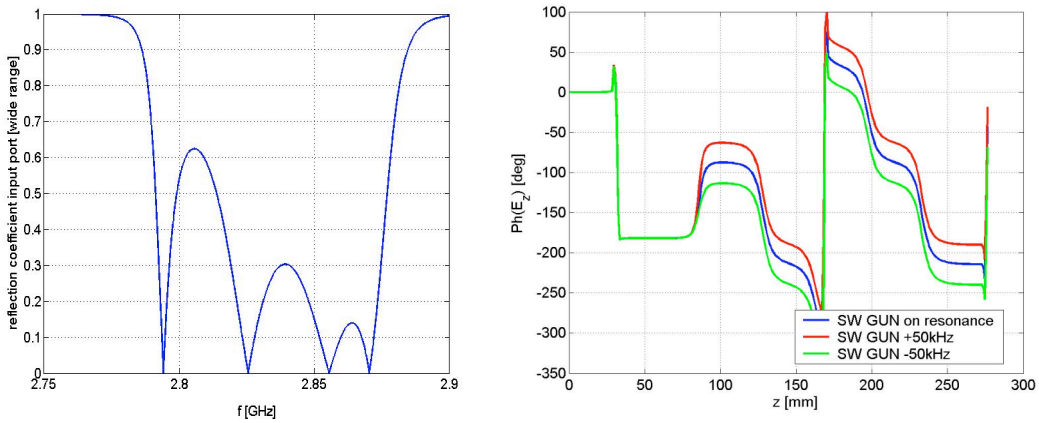

Figure 3. (left) Reflection from HFSS model of hybrid photoinjector in Fig. 27; (right) RF phase in structure sensitivity study.

Beginning in 2004, the UCLA/URLS collaboration recommenced work on this subject. As a first step at URLS, the matching of an X-band 2π/3-mode traveling wave structure to correct external coupling was studied. Subsequently at UCLA, this coupler design was adapted to S-band, and then the SW "gun" section, which is very close in geometry to the standard high gradient S-band gun at UCLA, was successfully added,

as illustrated in Fig. 2. In parallel, the URLS team has been developing a similar design in X-band. These efforts are heavily based on HFSS simulations, which have allowed us to produce designs with $S_{11}< 0.1$ thus far, with the desired higher field in the gun with respect to the traveling wave section. Examples of the RF design work are shown in Figs. 2 and 3; a full discussion of the results of the S-band HFSS results, as well as cold-test development, are given elsewhere in these proceedings[7].

Figure 2 illustrates the accomplishment of desired fields in the respective TW and SW parts of the structure, with a difference in average acceleration in the two sections — it is 30 MV/m in the SW gun section (60 MV/m peak), and 14 MV/m in the TW section. Figure 3 shows the degree of RF matching in the structure, and the phase relationships between the SW and TW sections. Several aspects of the structure are visible from these results: the excellent matching at the π-mode resonance, the sensitivity of the TW v. SW phase as a function of temperature (indicating the level of control needed). The structure is well matched after the SW section fill time, with only slight difference found during the fill. This is because the gun uses only ~10% of the total power, and the reflected wave from it during the fill is shared between going bacl towards the source, and propagating downstream in the TW section.

Even more importantly, one sees from Fig. 3 that the phase advance between the gun section "full cell" and the downstream coupling cell is only 90º. This is *not* the phase for optimal acceleration, but is instead the phase demanded by velocity bunching. This fortuitous state of affairs leads to predictions of very high current, low emittance beams being formed in the hybrid.

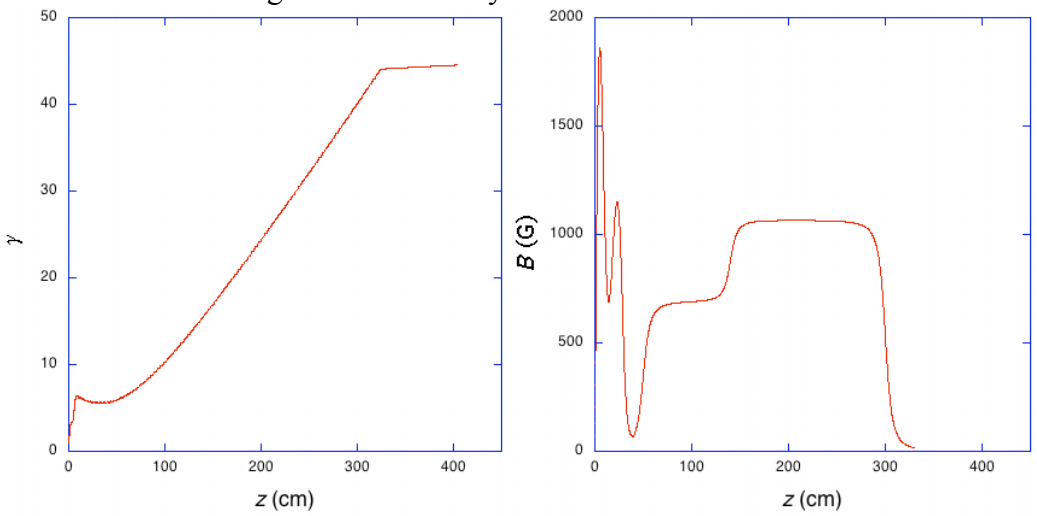

Figure 4. (left) Acceleration scheme simulated (UCLA PARMELA) in hybrid photoinjector showing initial slight deceleration; (right) solenoid field profile associated with focusing scheme.

BEAM DYNAMICS SIMULATIONS

The beam dynamics in this device, in which the TW section is lengthened to L_{TW}=3 m, have been explored using UCLA PARMELA. In this scenario, a peak power of 25 MW is needed to drive the structure. A beam of Q=1 nC, with radius R_b=1.57, mm, and total bunch length 10 psec, is launched at central phase ϕ_0=40º into the RF environment described above, and focused (Fig. 4) using the primary solenoids

shown in Fig. 1, as well as additional solenoids wrapped about the TW sector. Initial deceleration is noted after the coupling cell where the beam is ~4 MeV, followed by an optimized acceleration program typical of a velocity bunching, in which the beam is first compressed, and then the energy spread is mitigated. This mitigation is accomplished by accelerating the beam slightly back of RF crest — the need to run at this asymptotic phase is drives the choice of initial decelerating phase.

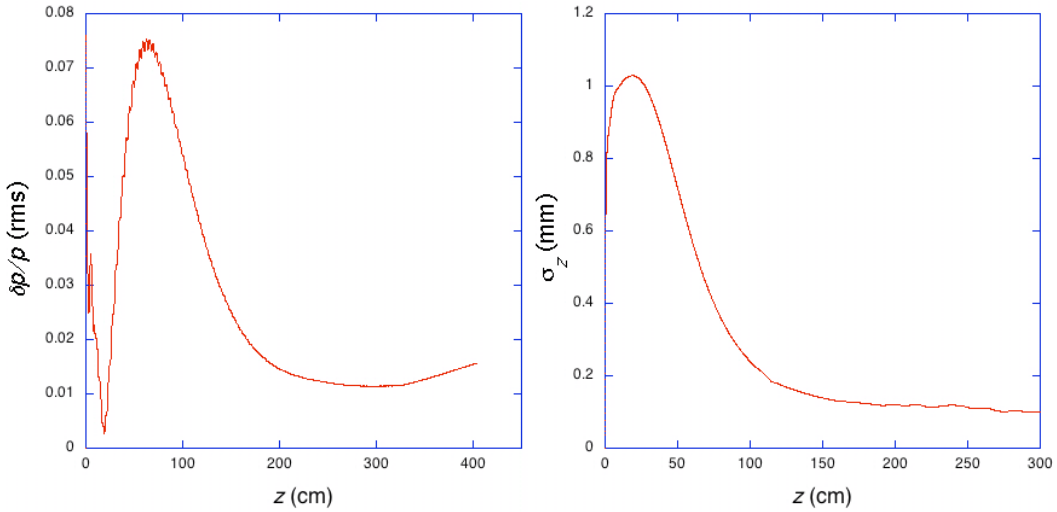

Figure 5. (left) Simulated evolution of momentum spread in hybrid photoinjector; (right) evolution of rms bunch length in hybrid.

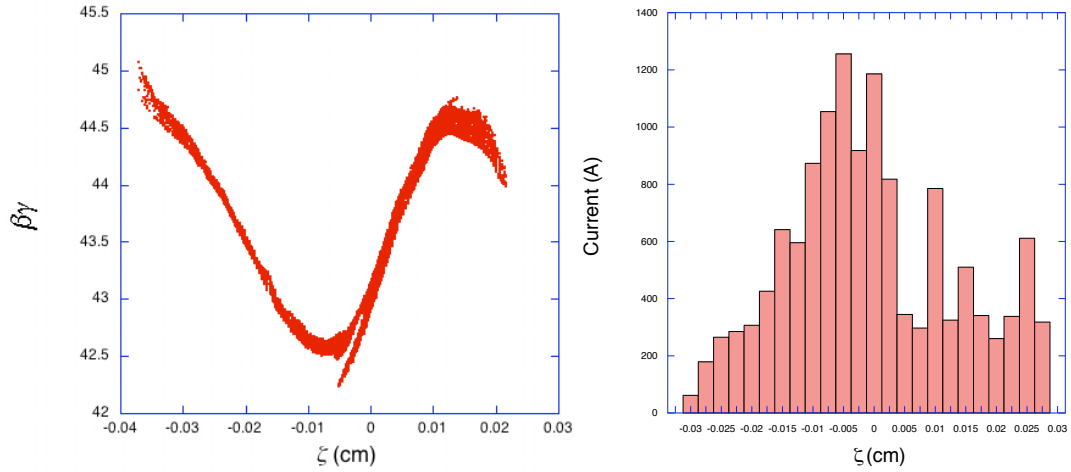

Figure 6. (left) Simulated final longitudinal in hybrid photoinjector; (right) associated current profile.

The evolution of both the momentum spread and the rms bunch in the hybrid are shown in Fig. 5. The rms bunch length shortens from > 1 mm to less than 100 μm, or 1.2 kA peak current, as illustrated in Fig. 6. The momentum spread undergoes a minimum of ~1% at the structure exit, but expands due to space charge downstream that arises from the very high peak current. Figure 6 also shows the final longitudinal phase space of the velocity-bunched beam, which displays a characteristic folded shape. This signature in the phase space is a result of the interplay between RF compression and defocusing longitudinal space charge forces.

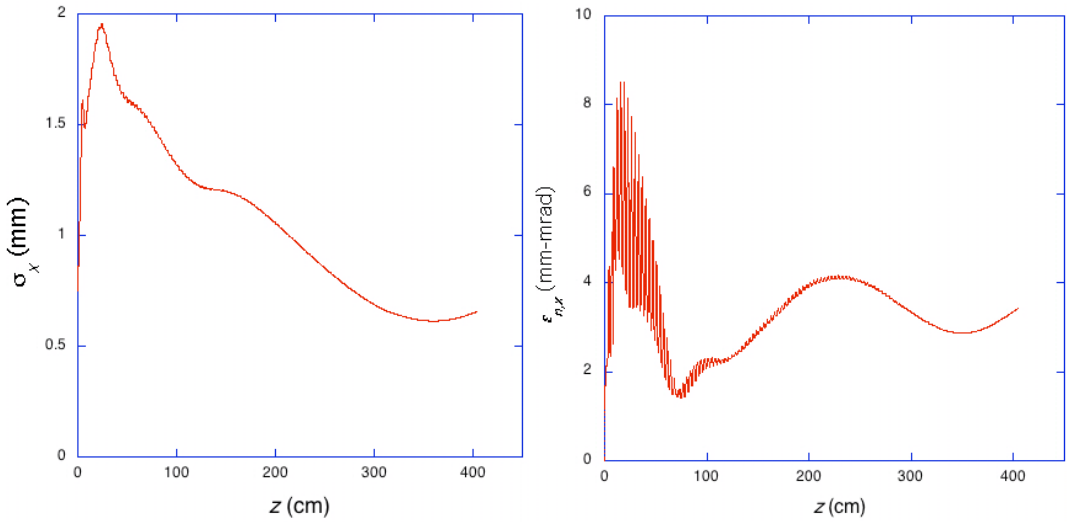

Figure 6. (left) Simulated evolution of transverse rms bunch size in hybrid photoinjector; (right) evolution of rms normalized emittance in hybrid.

The rms bunch size is well controlled during velocity bunching by the addition of solenoid focusing over the TW section. The relatively strong oscillations in the emittance driven by the increasing space charge forces are fairly well controlled, with a minimum of 3 mm-mrad (rms normalized) predicted at the structure exit. Much of the emittance can be eliminated by collimation of small charge in the beam tail; the rms emittance can be halved by removing only 15% of the outlying charge. We note, however, that one should use this high current beam within a short distance downstream of hybrid photoinjector exit.

STATUS AND FUTURE PLANS

At present, a cold-test model of the S-band structure shown in Fig. 2 has been machined at UCLA, and is now undergoing low-level RF tests. This is a critical phase, as the simultaneous measurement and tuning of both SW and TW characteristics remains a challenge. The RF design of the cold-test model and initial measurements on the device are described in detail in Ref. ?.

Final photoinjector-related work is now underway to identify designs for laser injection assemblies and focusing solenoids. The present design calls for introducing a cut in the solenoid placed over the first SW "gun" cell, in which a laser is injected at ~62º through the joint between the cell outer wall and the first iris. When the envelope of the full structure is specified, we will proceed to re-examine the beam dynamics (little is expected to change in this regard, as the solenoid field profile should be reproduced), and to design the cooling circuit, which will be split into SW and TW regions to stabilize the phase sensitivity shown in Fig. 3.

Within one year, we plan to fabricate a long, high power version of the hybrid, and test this structure at the UCLA PEGASUS laboratory. After commissioning of this device, we then plan to use the extremely bright beam produced in it for radiation production, considering both coherent Cerenkov wake and FEL devices, and incoherent X-ray production from inverse Compton scattering (ICS).

The end goal of producing coherent, narrow band radiation at UCLA is to use the emitted power to drive slab-symmetric accelerator structures[8,9] in the THz band at the Neptune Advanced Accelerator Lab. In the case of the FEL, we consider the following parameters: undulator wavelength $\lambda_u = 7.6$ cm, peak undulator field $B_u = 7.9$ kG, and undulator length $L_u = 80$ cm. In this case, we estimate that the output power from an FEL operating at 340 μm wavelength in the super-radiant mode[10] to be ~30 MW.

On the other hand, similar results can be obtained by using coherent Cerenkov radiation from a fused silica tube, as discussed in Ref. 11. Assuming an inner radius a=250 μm and an outer radius b=375 μm, a power of ~15 MW is generated at 700 μm wavelength. While the use of this simple tube to create coherent radiation has obvious practical advantages, it has drawbacks as well. First, the radiation is radially polarized, and therefore a mode conversion procedure would need to be performed for use in the type of structure described in Refs. 8 and 9. Second, the mode content is not pure, and many harmonics are produced, at a much higher power level than in the FEL.

The production of X-rays from the ICS process using the hybrid requires focusing of the beam to a very small spot. With the desire to create even shorter X-ray pulses also considered, the scaled X-band version of the hybrid under study at URLS and LNF is perhaps even more compelling. The scaling laws of Ref. 1 allow us to predict the performance of the device: the peak on-axis electric field in the SW section will be 240 MV/m, corresponding to 50 MW of 11.4 GHz power; with the charge scaled also as $Q \propto \lambda_{RF}$, one may anticipate a 0.25 nC beam with 1.2 kA (80 fsec rms) and ε_n~0.75 mm-mrad. In 180º scattering geometry with an 800 nm laser, this beam would produce ICS photons with 1Å wavelength, thus allowing it to reproduce the wavelength and time structure of an X-ray FEL, albeit with incoherent light.

ACKNOWLEDGMENTS

This work was performed under the auspices of the U.S. Department of Energy under contract numbers DE-FG-98ER45693 and DE-FG03-92ER40693.

REFERENCES

1. J.B. Rosenzweig and E. Colby, *Advanced Accelerator Concepts* p. 724 (AIP Conf. Proc. 335, 1995).
2. Dennis T. Palmer, "The next generation photoinjector," Stanford University dissertation, 1998.
3. R.L. Sheffield, E.R. Gray, J.S. Fraser, *Nucl. Inst. Meth.* A272 **222**, (1988).
4. X. Ding "The PWT Photoinjector", PhD thesis, UCLA, 2000.
5. D. Yu *et al*. in *Proc. of the 1999 Particle Accelerator Conf*., 2003 (IEEE, 1999).
6. S. Telfer, in *Proc. of the 2003 Particle Accelerator Conf*., 2120 (IEEE, 2003).
7. B. O'Shea, *et al*., these proceedings.
8. J.B. Rosenzweig, A. Murokh, and C. Pellegrini, *Phys. Rev. Letters* **74**, 2467 (1995).
9. R. B. Yoder* and J. B. Rosenzweig *Phys. Rev. ST Accel. Beams* **8**, **111301** (2005)
10. A. Gover, Phys. Rev. ST Accel. Beams 8, 030701 (2005)
11. A. Cook, et al., these proceedings.